



OPEN ACCESS

EDITED BY

Rajesh MK,
Central Plantation Crops Research Institute
(ICAR), India

REVIEWED BY

Fangcheng Bi,
Guangdong Academy of Agricultural
Sciences, China
Raviraj M. Kalunke,
Donald Danforth Plant Science Center,
United States

*CORRESPONDENCE

Yu-Liang Cai
✉ yuanyicyl@nwsuaf.edu.cn

SPECIALTY SECTION

This article was submitted to
Plant Pathogen Interactions,
a section of the journal
Frontiers in Plant Science

RECEIVED 22 December 2022

ACCEPTED 02 February 2023

PUBLISHED 09 February 2023

CITATION

Pan L-Y, Zhou J, Sun Y, Qiao B-X, Wan T,
Guo R-Q, Zhang J, Shan D-Q and Cai Y-L
(2023) Comparative transcriptome and
metabolome analyses of cherry leaves spot
disease caused by *Alternaria alternata*.
Front. Plant Sci. 14:1129515.
doi: 10.3389/fpls.2023.1129515

COPYRIGHT

© 2023 Pan, Zhou, Sun, Qiao, Wan, Guo,
Zhang, Shan and Cai. This is an open-access
article distributed under the terms of the
[Creative Commons Attribution License
\(CC BY\)](https://creativecommons.org/licenses/by/4.0/). The use, distribution or
reproduction in other forums is permitted,
provided the original author(s) and the
copyright owner(s) are credited and that
the original publication in this journal is
cited, in accordance with accepted
academic practice. No use, distribution or
reproduction is permitted which does not
comply with these terms.

Comparative transcriptome and metabolome analyses of cherry leaves spot disease caused by *Alternaria alternata*

Liu-Yi Pan¹, Jing Zhou¹, Yan Sun¹, Bai-Xue Qiao¹, Tian Wan¹,
Rui-Quan Guo¹, Juan Zhang^{1,2}, Dong-Qian Shan¹
and Yu-Liang Cai^{1*}

¹College of Horticulture, Northwest A&F University, Yangling, Shaanxi, China, ²College of Horticulture and Forestry, Tarim University, Alar, Xinjiang, China

Alternaria alternata is a necrotrophic fungal pathogen with a broad host range that causes widespread and devastating disease in sweet cherry (*Prunus avium*). We selected a resistant cultivar (RC) and a susceptible cultivar (SC) of cherry and used a combined physiological, transcriptomic, and metabolomic approach to investigate the molecular mechanisms underlying the plant's resistance to *A. alternata*, of which little is known. We found that *A. alternata* infection stimulated the outbreak of reactive oxygen species (ROS) in cherry. The responses of the antioxidant enzymes and chitinase to disease were observed earlier in the RC than in the SC. Moreover, cell wall defense ability was stronger in the RC. Differential genes and metabolites involved in defense responses and secondary metabolism were primarily enriched in the biosynthesis of phenylpropanoids, tropane, piperidine and pyridine alkaloids, flavonoids, amino acids, and α -linolenic acid. Reprogramming the phenylpropanoid pathway and the α -linolenic acid metabolic pathway led to lignin accumulation and early induction of jasmonic acid signaling, respectively, in the RC, which consequently enhanced antifungal and ROS scavenging activity. The RC contained a high level of coumarin, and *in vitro* tests showed that coumarin significantly inhibited *A. alternata* growth and development and had antifungal effect on cherry leaves. In addition, differentially expressed genes encoding transcription factors from the MYB, NAC, WRKY, ERF, and bHLH families were highly expressed, they could be the key responsive factor in the response of cherry to infection by *A. alternata*. Overall, this study provides molecular clues and a multifaceted understanding of the specific response of cherry to *A. alternata*.

KEYWORDS

transcriptome, metabolome, cherry leaves, *Alternaria alternata*, defensive response

1 Introduction

The sweet cherry (*Prunus avium* L.) industry has expanded rapidly in recent years with the development of numerous cultivars and is of high economic importance in temperate regions worldwide (Wünsch and Hormaza, 2002). Despite the expansion of cherry cultivation areas, diseases caused by pests have become one of the main factors restricting advances in the cherry industry (Pasquariello et al., 2015). Cherry black spot is a common fungal disease caused by the pathogen *Alternaria alternata*, which mainly damages leaves and fruits (Yang et al., 2020; Pan et al., 2022). The disease occurs during the hot and rainy conditions in summer and autumn and can reach a rate of 60–100%. The severely diseased leaves all fall off their trees from August to September, directly affecting the tree's vegetative growth post-harvest for that year, as well as flower bud differentiation and yield for the following year. The disease lesions are small black circular spots that gradually expand to 3–5 mm in diameter. These spots may coalesce or continue to expand, becoming irregular and darker in color (Thomidis and Tsipouridis, 2006). Black spot disease has been studied in several plants, including pear (Yang et al., 2015), citrus (Gai et al., 2019), and marigold (Cheng et al., 2019). However, research on cherry black spot disease is limited, with investigations focused on pathogen isolation, identification, and chemical control. Currently, the measures for preventing and controlling cherry diseases mainly include chemical pesticide application. Although these pesticides can reduce the probability of disease occurrence, they are environmental pollutants. Moreover, the various types and dosages of pesticides can result in drug-resistant pathogens, thus increasing the difficulty of control (Li et al., 2022). Therefore, a better understanding of the defense mechanism of cherry against *A. alternata* will help develop innovative and safer control strategies. Additionally, breeding and utilizing disease-resistant cultivars will increase their selectivity and reduce their dependence on chemical agents for disease management.

Plants have evolved to form complex and efficient protective mechanisms against the invasion of pathogenic bacteria, including cytoplasmic membrane phosphorylation, activation of cytoplasmic kinases, stimulation of reactive oxygen species (ROS) production, activation of Ca²⁺ channels, promotion of protein translation, and production of secondary metabolites, which ultimately result in immune responses in plants (Cohn et al., 2001; Schwessinger and Ronald, 2011). High-throughput sequencing technology is a next-generation sequencing technology widely used in plant disease research. Metabolomics is used to reflect the synthesis, decomposition, and transformation of all or certain types of metabolites in an organism's tissue or cell (Hall, 2011; Khakimov et al., 2014). Transcriptomics and metabolomics have been used to study fungal interactions with non-model plant hosts, including soybean (Ranjan et al., 2019), jujube fruit (Yuan et al., 2019) and apple (Zhou et al., 2019). Biological stress is associated with reprogramming many defense-related genes and transcription factors. For example, citrus fruit inhibit *Penicillium digitatum* infection by enhancing ERF, WRKY, and MYB transcription, as well as the transcription of genes encoding stress, thus accumulating rhamnose and inositol (Ning et al., 2018). Gao et al. (2016) found that the response of peach trees to *Lasiodiplodia theobromae* infection was related to the expression of genes related

to phenylpropanoid biosynthesis and glycometabolism. Abdelrahman et al. (2020) found that disease-resistant wild *Asparagus kiusianus* showed specific metabolic changes with increased flavonoids and steroidal saponins content. By contrast, limited information is available on the physiological and molecular response mechanism of cherry resistance to *A. alternata*, which would be the basis for successful disease resistance breeding. Therefore, the co-expression analysis of differential genes and metabolites via combined transcriptomic and metabolomic studies could be used to explore the causal relationship between genes and metabolites. Locking the key metabolic pathways and identifying candidate disease resistance genes may be an effective method to better explore and understand the mechanism of disease resistance in cherry to *A. alternata*.

The incidence and severity of leaf spot disease caused by *A. alternata* vary according to the cherry cultivar. We previously investigated different cherry cultivars for resistance to the natural incidence of the disease in the field and found that *P. cerasus* 'Aode' showed high resistance, while *P. avium* 'Rita' showed high sensitivity (data unpublished). Schuster and Tobutt evaluated the resistance of cherry genotypes to leaf spot disease and found tart cherry cultivars to be resistant and all tested sweet cherry cultivars to be susceptible (Schuster and Tobutt, 2004). Therefore, in the present study, we used the germplasm of cherry cultivars with marked differences in disease resistance as the research material to measure the physiological changes of cherry leaves during infection. Furthermore, we used transcriptome and metabolome sequencing to analyze the plant defense response pathways involving differentially expressed genes (DEGs) and differentially accumulated metabolites (DAMs), thereby revealing the potential defense mechanism of cherry against infection with *A. alternata*. The findings of this study could provide different perspective into how hosts fight the onslaught of fungal infections and accelerate the development and selection of resistant cherry cultivars.

2 Materials and methods

2.1 Plant materials and inoculation treatment

We selected *P. avium* 'Rita' (susceptible cherry cultivar (SC)) and *P. cerasus* 'Aode' (resistant cherry cultivar (RC)) as experimental materials. Among them, 'Rita' originated in Hungary and its parent is Trusenzskaja 2 × H2 (Germersdorfer open pollination) (Iličić et al., 2018), 'Aode' is a new sour cherry cultivar derived from wild sour cherry by seedling selection in China (Cai et al., 2014). One-year-old two selected cultivars grafted on *P. mahaleb* CDR-1 rootstocks were planted in the greenhouse at Northwest A&F University, Yangling, Shaanxi, China (34°20' N, 108°24' E). All test materials were maintained in the same growth state, grew robustly, and showed no pest infestation or diseases. The pathogen was isolated from diseased cherry leaves, and the isolate was confirmed to be *Alternaria alternata* via morphological culture characterization and molecular identification. *A. alternata* was incubated on potato dextrose agar (PDA) medium for 7 days at 25°C. The fourth and fifth open cherry leaves from the shoot tips were infected with a plaque of actively growing fungus (3 mm in diameter; excised using a punch to maintain consistency). Each leaf was inoculated with six pieces of fungus plaque

(Zhu et al., 2017; Hu et al., 2018). Plant tissue was collected at the junction of diseased and healthy leaves using a clean straight-edged razor at 0, 1, 3, 5, 7, and 9 days post inoculation (dpi). The three biological replicates used for each treatment group.

2.2 Field emission scanning electron microscope observation of infected tissue

The morphology of cherry leaves inoculated with *A. alternata* was observed according to the method described by Liang et al. (Liang et al., 2020). The morphology of leaf tissue at 5 dpi was observed using FESEM (Hitachi, Tokyo, Japan). The cherry leaves were washed and cut into slices (length \leq 5 mm, thickness \leq 3 mm). Each slice was immersed and fixed in 4% (v/v) glutaraldehyde for more than 2 hours. Next, the slices were washed with 0.1 M PBS buffer (pH 6.8) four times, then washed with 30%, 50%, 70%, 80%, and 90% ethanol and washed three times with 100% ethanol. The ethanol was replaced with isoamyl acetate once. Finally, the tissue samples were dry gold plated and observed *via* FESEM.

2.3 Determination of the physiological index of cherry leaves

Different crude enzyme solutions from leaf tissue (0.2 g) were extracted using 5 mL of different extraction buffers. Sodium borate buffer (pH 8.8) containing 40 g/L polyvinylpyrrolidone (PVP) and 0.1 mol/L acetate-sodium acetate buffer (pH 5.5) was used for PPO and POD extraction. Sodium phosphate buffer (0.1 mol/L; pH 7.8) was used for SOD and CAT extraction. The activities of PPO, POD, CAT, and SOD were determined according to our previously reported method (Pan et al., 2020; Pan et al., 2022). The activities were expressed as U/g based on fresh weight.

The MDA content was determined according to the method described by Dhindsa et al. (1981) with slight modifications. Cherry leaf samples (each 0.1 g) were homogenized in 5 mL of 5% (w/v) cold trichloroacetic acid solution, and centrifuged at 10,000 rpm for 10 min. Next, 2 mL of thiobarbituric acid was added to 2.0 mL of supernatant, and the reaction tubes were transferred to a boiling water bath for 20 min. The mixture was rapidly cooled and centrifuged again, and OD values were obtained at 420 nm, 532 nm, and 600 nm using a spectrophotometer.

The H₂O₂ content was determined using an assay kit (Beijing Soleibo Technology Co., Ltd., China) according to the manufacturer's instructions. The H₂O₂ content was calculated on the basis of standard H₂O₂ at an absorbance of 415 nm and expressed as $\mu\text{mol}\cdot\text{g}^{-1}\text{FW}$.

The activities of CHI and GLU in cherry leaves inoculated with *A. alternata* were determined using the indicated kits (Beijing Solarbio Technology Co., Ltd.) according to the manufacturer's instructions. Absorbance was measured at 585 nm and 540 nm using a full-wavelength multi-function microplate reader (Tecan Infinite M200pro, Switzerland). The result was expressed as U/g based on fresh weight.

The lignin content in cherry leaves inoculated with *A. alternata* at 0, 1, and 5 dpi was determined using the indicated kit (Beijing Solarbio Technology Co., Ltd.) according to the manufacturer's instructions.

2.4 Transcriptome sequencing analysis

Cherry leaves at 0, 1, and 5 dpi after inoculation with *A. alternata* were used for RNA extraction, with three biological replicates per treatment. The raw data were obtained using the Illumina Novaseq6000 sequencing platform by Gene Denovo Biotechnology Co., Ltd. (Guangzhou, China). The paired-end clean reads were mapped to the cherry reference genome using HISAT2. 2.4 (Kim et al., 2015; Wang et al., 2020). Mapped reads for each sample were assembled using StringTie v1.3.1 (Pertea et al., 2015; Pertea et al., 2016), and RSEM was used to normalize gene transcription level to FPKM. We used DESeq2 (Love et al., 2014) to screen DEGs with false discovery rate (FDR) below 0.05 and $|\log_2(\text{fold change})| \geq 2$. DEGs were mapped to Gene Ontology (GO) and Kyoto Encyclopedia of Genes and Genomes (KEGG) databases to further analyze biological functions and key metabolic pathways.

2.5 Widely targeted metabolome analysis

Eighteen cherry leaf samples (each treatment included three biological replicates) were crushed using a mixer mill (MM 400, Retsch) at 30 Hz for 1.5 minutes. Next, 100 mg of cherry leaf powder was extracted with 70% aqueous methanol, and the extracted compounds were analyzed using an LC-ESI-MS/MS system (Chen et al., 2013). Data were filtered, detected peaks, aligned, and calculated using Analyzer 1.6.1. The DAMs between two groups were determined by $P < 0.05$ for the T-test and $\text{VIP} \geq 1$. Next, a DAM pathway enrichment analysis was performed *via* the KEGG database.

2.6 Association analysis of transcriptome and metabolome data

The disease resistance responses of differential genes and differential metabolites of RC and SC were simultaneously mapped to the KEGG pathway database using GenMAPP v2.1 to obtain information about their common pathways.

2.7 RT-qPCR verification

RNA was reverse transcribed using the cDNA synthesis SuperMix kit (Yeasen Biotech Co., Ltd., Shanghai, China). RT-qPCR was performed using our previous method (Pan et al., 2022). Gene-specific primers were listed in Table S9. All reactions included three biological replicates. The relative gene expression level was calculated according to the $2^{-\Delta\Delta\text{CT}}$ method (Livak and Schmittgen, 2002), with *P. avium* actin gene as an internal standard.

2.8 Plate inhibition assay of *A. alternata*

Growth inhibition assays of *A. alternata* were performed on culture plates using the growth rate method. PDA medium was prepared using 0 (blank control), 250, 500, or 1000 $\mu\text{g/mL}$ of phenylalanine or tyrosine and DMSO (dimethyl sulfoxide) as the

control solvent. PDA medium with DMSO was also used as a control to exclude the effect of DMSO on the experiment. The plates were inoculated with active *A. alternata* and grown at 25°C for 7 days to assess colony diameter. The assay was repeated three times for each concentration, and the inhibitory rate was calculated as follows: inhibitory rate = [(colony diameter of control – colony diameter of treatment)/colony diameter of control] × 100%.

2.9 Effect of coumarin on mycelial growth of *A. alternata* in cherry leaves

The 500 µg/mL coumarin solution was evenly sprayed on the surface of RC leaves, and then *A. alternata* was inoculated, the inoculation method is the same as described in Section 2.1. In order to improve the effect of coumarin, the leaves were moisturized with transparent preservative bags for 24 h. The lesion diameter was observed and measured at 5 dpi.

3 Results

3.1 Changes in symptoms following *A. alternata* infection

P. avium ‘Rita’ (SC) and *P. cerasus* ‘Aode’ (RC) were selected based on our previous evaluation of different cherry cultivars for resistance to *A. alternata*. At 1 dpi with *A. alternata*, initial symptoms began appearing in the susceptible cultivar as light brown spots around the inoculation site that spread with the disease progressed, a darkening of the color was observed at the infection site at 5 dpi (Figure 1A). By contrast, lesion enlargement was limited on the leaves of the RC cultivar (Figure 1B). We measured the development of

lesion diameter after inoculation with *A. alternata*, the lesion diameter of RC was only 63.14% of SC at 5 dpi and was significantly smaller than SC throughout the infection process (Figure S1). The inoculated leaves were observed using a FESEM, and the germination rate of conidia of the pathogen was higher on the leaf surface of the SC at 5 dpi. Moreover, a higher number of germ tubes—formed *via* spore germination—directly invaded the host tissue, and more mycelia entered the infected tissue *via* the stomata (Figure 1C). Conversely, the germination rate of conidia was significantly reduced in the RC leaf. Only scattered hyphae and single conidia were detected, and few germ tubes were produced (Figure 1D).

3.2 Physiological changes in cherry leaves inoculated with *A. alternata*

Antioxidant enzymes can transform peroxides in the plant into less toxic or harmless substances. Here, peroxidase (POD), polyphenol oxidase (PPO), and superoxide dismutase (SOD) activities in the RC were significantly higher than those in the SC at the early stage of *A. alternata* inoculation, whereas the response of the SC to pathogenic fungi occurred after 5 dpi. Catalase (CAT) activity was significantly higher in the SC than in the uninoculated leaves (except at 3 dpi) and accumulated significantly in the RC at 1 dpi before leveling off. Following inoculation with *A. alternata*, the hydrogen peroxide (H₂O₂) content of the SC was significantly higher than that of the uninoculated group, while the H₂O₂ content of the RC was significantly higher than that of the uninoculated group at 1–3 dpi, suggesting that H₂O₂ accumulation was induced by pathogen infection (Figure 2).

The malondialdehyde (MDA) content of the SC showed an upward trend with the extension of infection time and increased

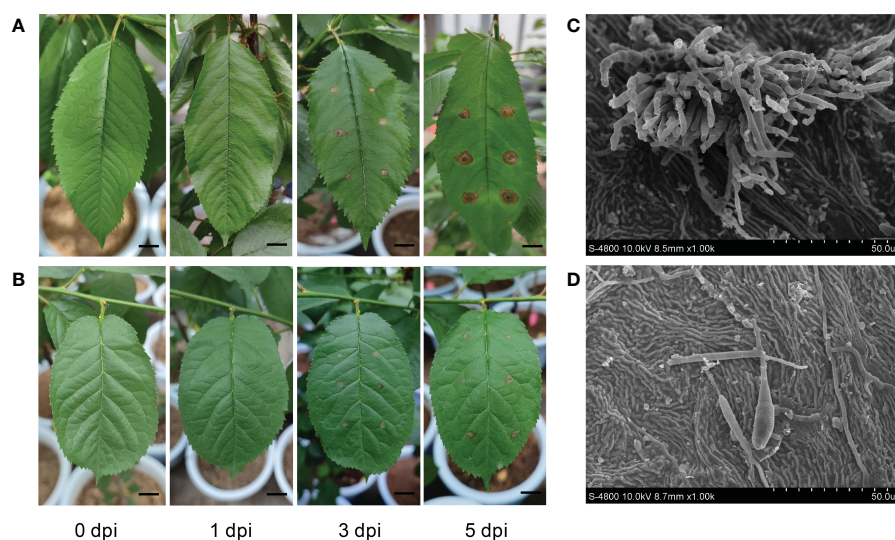


FIGURE 1

Analysis on symptoms and physiological indexes of *Alternaria alternata* infection in susceptible cultivar (SC) and resistant cultivar (RC). Disease symptoms of the (A) SC and (B) RC were observed following leaf inoculation with actively growing mycelia of *A. alternata* at 0, 1, 3, and 5 days post inoculation (dpi); scale bar = 10 mm. (C) Images showing infection in the SC at a magnification of x1.00 k at 5 dpi. (D) Images showing infection in the RC at a magnification of x1.00 k at 5 dpi.

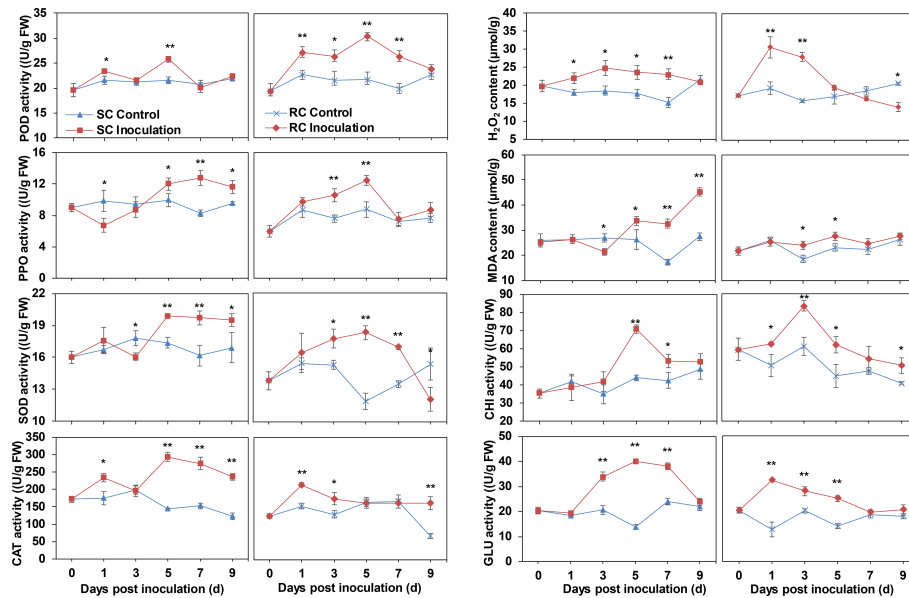


FIGURE 2

Determination of physiological indexes related to disease resistance, including peroxidase (POD), polyphenol oxidase (PPO), superoxide dismutase (SOD), catalase (CAT) enzyme activity, hydrogen peroxide (H_2O_2) and malondialdehyde (MDA) content, chitinase (CHI) and β -1,3 glucanase (GLU) enzyme activity. Error bars represent standard deviation ($n = 3$). * indicates a significant difference at p -value < 0.05 , ** indicates a significant difference at p -value < 0.01 .

sharply, especially after 5 dpi. By contrast, the content of MDA in the RC changed little during the infection process and had significantly difference with control only at 3, and 5 dpi (Figure 2).

In addition, the chitinase (CHI) and β -1,3 glucanase (GLU) activities were up-regulated after cherry leaves were infected by *A. alternata* (Figure 2). However, activity in the RC was significantly higher than in the uninoculated leaves during the early stage of inoculation but significantly higher in the SC than the control during the later stage of inoculation. Therefore, we speculated that resistance was induced and responded by the fungal pathogen earlier in the RC than the SC.

We considered that the resistance of cherry leaves to *A. alternata* may be more sensitive in the early stage of infection, based on data obtained on the physiological changes of cherry leaves following inoculation with *A. alternata*, in conjunction with leaf disease development. Therefore, cherry leaves were collected for transcriptome and metabolome determination at 0, 1, and 5 dpi.

3.3 Transcriptomic analysis of cherry in response to *A. alternata*

3.3.1 Overview and analysis of transcriptome sequencing data

RNA-seq data were generated from nine RC and nine SC samples at different stages (0, 1, and 5 dpi). A total of 931,889,502 clean reads were obtained after filtering and removing adapter sequences and low-quality reads, and the percentages of GC and Q20 were 45.28–46.31% and 98.06–98.32%, respectively (Table S1). Correlation matrix analysis showed that the biological duplication was satisfactory and suitable for subsequent analysis (Figure 3A).

3.3.2 DEGs analysis of cherry in response to *A. alternata* infection

The gene expression level was estimated using the gene expression abundance corresponding to the FPKM value, and differential gene analysis was performed with $P < 0.05$ and $|\log_2FC| \geq 2$ as the screening criteria. The sequencing results showed 10,645 DEGs in the RC and SC during the infection process. A pairwise comparison of DEGs was performed between the RC and SC at specific time points, and 2315 and 2053 DEGs were identified at 0 dpi and 1 dpi, respectively; the number of DEGs increased sharply after 5 dpi (Figure 3B). Among these, 6445 DEGs were differentially regulated in both the RC and SC, 2117 DEGs were only found in the RC, and 2083 DEGs were only found in the SC (Figure 3C). Figure 3D shows the overlapping genes between these groups. These results indicate that *A. alternata* infection resulted in notable changes in cherry gene expression and significant differences between the RC and SC.

We mapped DEGs to Gene Ontology terms (<http://www.geneontology.org/>) to find significantly enriched GO entries. GO analysis revealed that DEGs were classified into three ontologies, including biological processes (BPs), molecular functions (MFs), and cellular components (CCs) (Figure S2). Most DEGs ($P \leq 0.05$) enriched in BPs were related to disease resistance, including the monoterpene metabolic process, phenylpropanoid metabolic process, phenylpropanoid biosynthetic process, jasmonic acid (JA) metabolic process, and hormone-mediated signaling pathway, at 1 and 5 dpi. MFs were mainly enriched in catalytic activity, oxidoreductase activity, and kinase activity, while CCs were mainly enriched in the extracellular region, cell periphery, external encapsulating structure, and cell wall (Table S2).

All DEGs were enriched to KEGG, and the enrichment pathways related to disease resistance were identified. DEGs between RC and

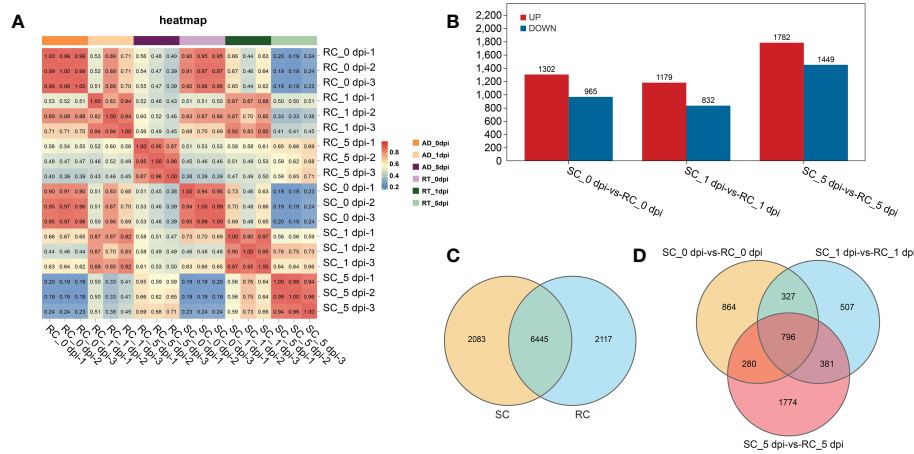


FIGURE 3 Analysis of the sample relationship and differentially expressed genes (DEGs) between groups. **(A)** Pearson correlation coefficients of all 18 samples; the correlation coefficients between the SC and RC were visually displayed as a heat map. **(B)** Up-regulation and down-regulation of DEGs. **(C)** A total of 2083 and 2117 DEGs were unique to the SC and RC, respectively. **(D)** DEGs in the SC compared to the RC at 0, 1, and 5 dpi.

SC were enriched in phenylpropanoid biosynthesis, α -linolenic acid metabolism, biosynthesis of secondary metabolites, tropane, piperidine and pyridine alkaloid biosynthesis, metabolite biosynthesis, glutathione metabolism, and amino sugar and nucleotide sugar metabolism in all three periods. Plant-pathogen interaction, flavonoid biosynthesis, and brassinosteroid biosynthesis were enriched at 0 and 1 dpi. Sesquiterpenoid and triterpenoid biosynthesis, phenylalanine, tyrosine and tryptophan biosynthesis were only enriched at 1dpi. DEGs were also enriched in photosynthesis, starch and sucrose metabolism, and cutin, suberin, and wax biosynthesis at 5 dpi (Figure 4). These results suggested that cherry has evolved various molecular defense reaction according to the infection stage of pathogenic fungi.

3.4 Metabolite profiling of cherry in response to *A. alternata*

3.4.1 Quality control of metabolomic data

Metabolome analysis was performed to determine the condition of the metabolites in the RC and SC after the occurrence of disease resistance. The widely targeted metabolite profiling of extracted disease-resistant and susceptible cherry samples was carried out using an LC-ESI-MS/MS system. A total of 1088 metabolites were detected and classified into 35 categories, among which the top three were phenolic acids, flavonols, and amino acids and derivatives (Table S3). A heatmaps were constructed by normalizing metabolite content (Figure S3A) and principal component analysis (PCA) was subjected.

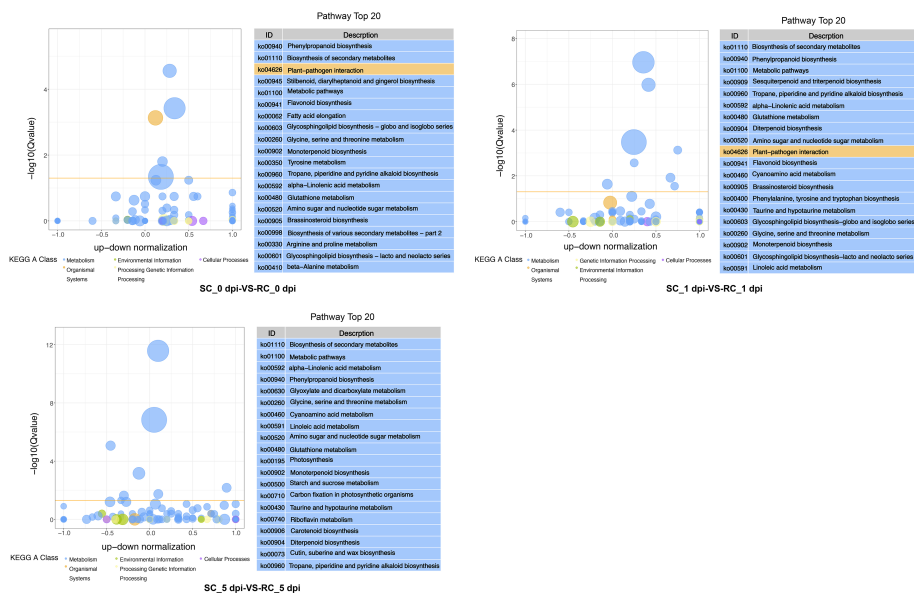


FIGURE 4 KEGG pathway analysis of pairwise comparisons (SC vs. RC) at 0, 1, and 5 dpi; the chart shows the top 20 pathways enriched in the selected group. The yellow line represents the threshold of $Qvalue=0.05$, and different colors represent different KEGG A class.

PC1 and PC2 explained more than 52.4% of the variability (Figure S3B). We used partial least squares discriminant analysis to analyze multivariate metabolite data (Figure S3C). The analysis showed that different metabolomic characteristics manifested at each time point during the infection process and that the resistant and susceptible materials showed a relatively large separation.

3.4.2 DAMs analysis of cherry in response to *A. alternata* infection

The DAMs between the two comparisons were screened by combining multivariate statistical analysis (OPLS-DA; VIP value) and univariate statistical analysis (T-test; P-value). The threshold for DAMs was $VIP \geq 1$ and $P < 0.05$. The number of up- and down-regulated DAMs was 48 and 58, respectively, in SC_0 dpi-vs-RC_0 dpi, 45 and 69, respectively, in SC_1 dpi-vs-RC_1 dpi, and 58 and 78, respectively, in SC_5 dpi-vs-RC_5 dpi, which increased with the extension of inoculation time (Figure S4). The top 10 DAMs that increased or decreased in each comparison group were identified by changes in metabolite accumulation (Figure S5).

Loading plots help to identify the metabolites that contribute the most to the changes in metabolite patterns between the comparison groups, i.e., the variables that contribute the most to the principal components of the OPLS model. Our findings showed that most DAMs far from the origin belonged to flavonoids and lipid metabolites (Figure 5A). The metabolites petunidin-3-O-(6''-O-p-Coumaroyl) glucoside, isorhamnetin-3-O-rutinoside, quercetin-5-O- β -D-glucoside, isohyperoside, L-Arginine, and coumarin were all far from the origin and contributed more to the discrimination between the two sample groups at the three time points. These are likely to be important variables leading to sample separation.

3.4.3 KEGG enrichment analysis of DAMs

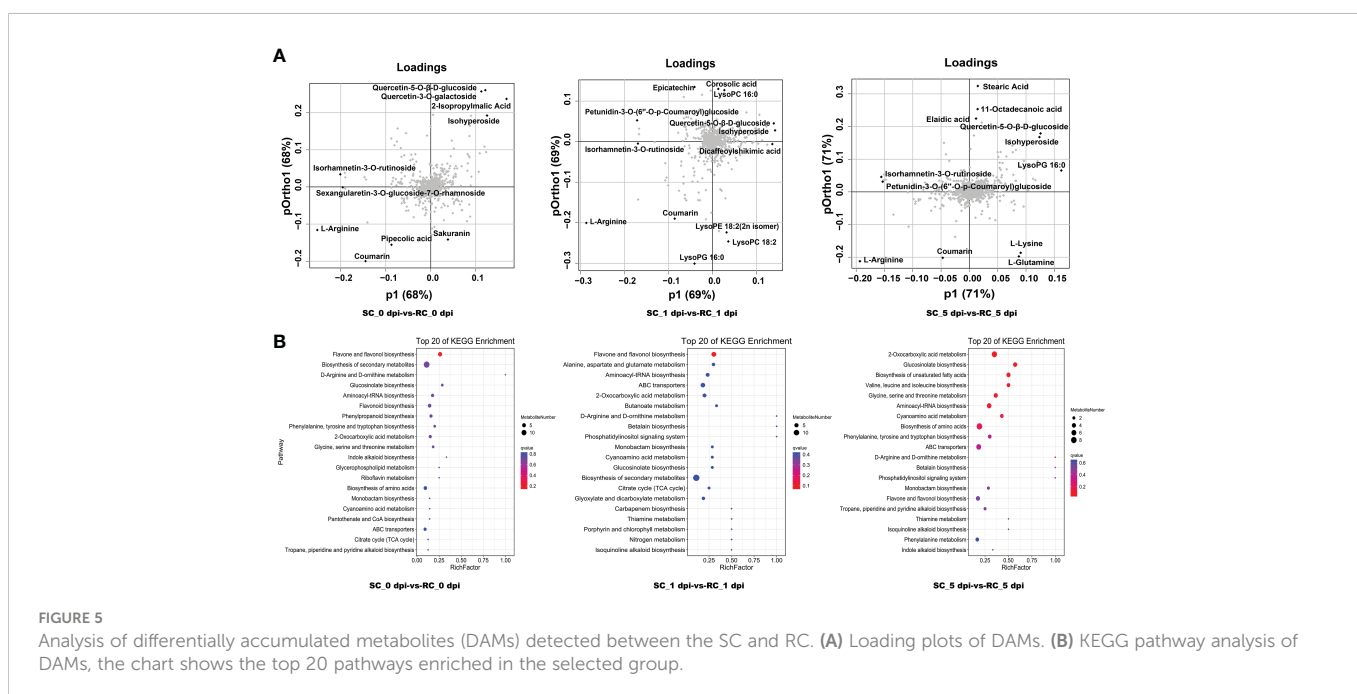
Based on the KEGG database annotations, we listed the top 20 paths enriched in each comparison group (Figure 5B). Among them,

DAMs were enriched in flavone and flavonol biosynthesis, ABC transporters, flavonoid biosynthesis, cyanoamino acid metabolism, tropane, piperidine and pyridine alkaloid biosynthesis, and phenylpropanoid biosynthesis, following inoculation with *A. alternata*. These metabolic pathways responded positively to the defense response of cherry. The results of enrichment analysis were consistent with those of transcriptome analysis. We noticed that only the metabolites kaempferol-3-O-galactoside and kaempferol-3-O-glucoside from flavone and flavonol biosynthesis were significantly up-regulated in the RC at all three stages, whereas the other flavonoid metabolites accumulated in the SC, which may suggest a specific response of the RC to *A. alternata* (Table S4).

3.5 Association analysis of transcriptome and metabolome data

3.5.1 Common metabolic pathway between genes and metabolites

We performed a combined transcriptome and metabolome analysis to understand further the mechanism of cherry resistance to *A. alternata* infection. KEGG enrichment analysis showed that comparisons of SC_0 dpi-vs-RC_0 dpi, SC_1 dpi-vs-RC_1 dpi, and SC_5 dpi-vs-RC_5 dpi had 31, 47, and 42 metabolic pathways mapped, respectively (Table S5). The main enriched metabolic pathways included phenylpropanoid biosynthesis, α -linolenic acid metabolism, flavonoid biosynthesis, biosynthesis of secondary metabolites, tropane, piperidine, and pyridine alkaloid biosynthesis, glutathione metabolism, ABC transporters, cyanoamino acid metabolism, and aminoacyl-tRNA biosynthesis. Considering that transcriptome analysis highlighted the important role of α -linolenic acid metabolism and phenylpropanoid biosynthesis in plant defense, we focused on these two metabolic pathways in subsequent analyses.



3.5.2 JA signaling in response to resistance against *A. alternata*

GO analysis indicated that DEGs between the RC and SC were significantly enriched in JA metabolism in biological processes at the transcript level (Table S2). KEGG analysis highlighted α -linolenic acid metabolic pathways associated with JA synthesis and response. The expression levels of three genes (FUN_008062, FUN_032051, and FUN_018478) encoding lipoxygenase (LOX) were up-regulated in the α -linolenic acid metabolic pathway. Two genes (FUN_017011 and FUN_004528) that encode allene oxide cyclase (AOC) were up-regulated in the RC during the early stage of *A. alternata* inoculation but down-regulated at 5 dpi, compared with the SC. In addition, the expression levels of one gene (FUN_029547) encoding hydroperoxide dehydratase (AOS) and nine genes encoding 12-oxophytodienoic acid reductase (OPR) were all down-regulated at 5 dpi (Figure 6A, Table S6). The RNA-seq data was validated via RT-qPCR (Figure 6B). Furthermore, JA content was significantly accumulated in the RC at 0 and 5 dpi. In addition, the accumulation of linolenic acid, a precursor of JA, was significantly less in the RC than in the SC at 5 dpi. Therefore, the differences in defense responses may be caused by different stages of *A. alternata* infection, and the sharp increase of key genes involved in JA synthesis at later stages in the SC may be considered a delayed response to the fungus.

3.5.3 The phenylpropanoid pathway in response to resistance against *A. alternata*

Plants have evolved various branched pathways for phenylpropanoid metabolism, producing numerous metabolites such as flavonoids, lignin, lignans, and cinnamic acid amides (Dong and Lin, 2021). Here, DEGs and DAMs related to the phenylpropanoid pathway were noticed between the RC and SC. We observed an up-regulation of genes encoding cinnamyl-alcohol

dehydrogenase (CAD), peroxidase (POD), caffeoyl-CoA O-methyltransferase (CCoAOMT), 4-coumarate-CoA ligase (4CL), cinnamoyl-CoA reductase (CCR), caffeic acid 3-O-methyltransferase (COMT), and scopoletin glucosyltransferase (TOGT) at the transcript level in RC compared to SC, as well as a down-regulation of genes encoding β -glucosidase (β -GLU) and shikimate O-hydroycinnamoyltransferase (HCT) (Figure 7A, Table S7). Furthermore, the lignin content of RC was significantly higher than that of SC at the early stage of inoculation (Figure 7B). Moreover, the gene expression of chalcone synthase (CHS) and flavonol synthase (FLS) related to flavonoid biosynthesis was significantly up-regulated in the RC compared to SC, following pathogen induction. Naringin and naringin chalcone also showed significant differences (Figure 6A). We selected candidate genes for RT-qPCR to validate the RNA-seq data, both sets of results were consistent (Figures S6A, B).

Based on the metabolomic data, we found that the metabolites phenylalanine, tyrosine, and coumarin were significantly accumulated in the RC compared with the SC (Figure 7A). Subsequently, plate inhibition assays of *A. alternata* showed that increasing concentrations of tyrosine and coumarin significantly inhibited the growth of *A. alternata* *in vitro*, while phenylalanine had no significant inhibitory effect on *A. alternata* (Figure 7C, Figure S7A). The inhibition rates of coumarin and tyrosine on the mycelial growth of *A. alternata* were significantly higher than that of phenylalanine, and the inhibition rates were 86.02% and 53.68% at the mass concentration of 1000 $\mu\text{g}/\text{mL}$, respectively (Figure S7B). Among them, coumarin had the most significant inhibitory effect on *A. alternata*, and we hypothesized that coumarin may inhibit the growth of diseased spots on cherry leaves. We then verified the effect of coumarin on mycelial growth of *A. alternata* in cherry leaves. The results showed that coumarin significantly inhibited the growth of diseased spots on RC leaves (Figures 7D, E).

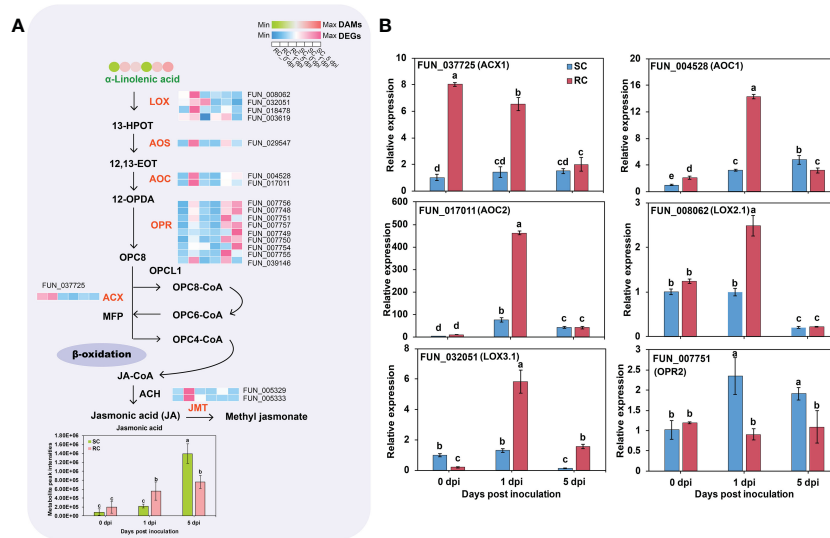


FIGURE 6
Jasmonic acid (JA) synthesis pathway and gene expression analysis. (A) Schematic representation of the core JA synthesis pathway; the circle heat map and the square heat map represent the expression of DAMs and DEGs, respectively, in the SC and RC at the three stages of testing. (B) RT-qPCR analysis of JA synthesis-related genes. Error bars represent standard deviation (n = 3). Different letters above the bars indicate significant differences at the 0.05 level according to Duncan's multiple range test.

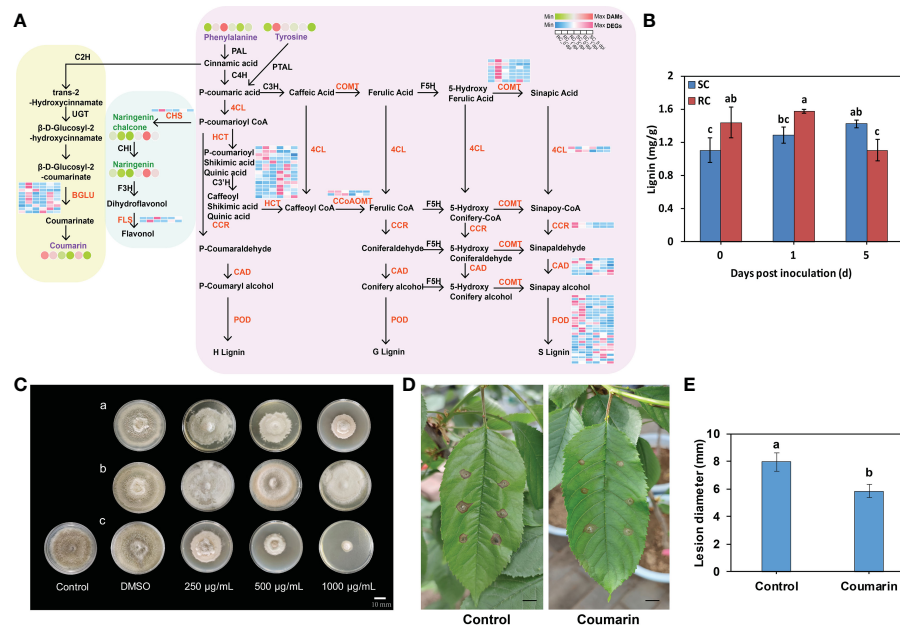


FIGURE 7

DEGs and DAMs involved in the phenylpropanoid pathway in the SC and RC inoculated with *A. alternata*. (A) Schematic representation of the core pathway of phenylpropanoid biosynthesis; the circle heat map and the square heat map represent the expression of DAMs and DEGs, respectively, in the SC and RC at the three stages of testing. (B) The lignin content of the SC and RC at 0, 1, and 5 dpi. Error bars represent standard deviation ($n = 3$). Different letters above the bars indicate significant differences at the 0.05 level according to Duncan's multiple range test. (C) Effect of the metabolites on *A. alternata* growth. Tyrosine (a) and coumarin (c) inhibit the growth of *A. alternata*, while phenylalanine (b) does not. DMSO (dimethyl sulfoxide) was used as the solvent control. Scale bar = 10 mm. (D) Effect of coumarin on growth of *A. alternata* in RC leaves. Scale bar = 10 mm. (E) Effect of coumarin on lesion diameter of RC leaves. Error bars represent standard deviation ($n = 3$). Different letters above the bars indicate significant differences at the 0.05 level according to Duncan's multiple range test.

3.6 Transcription factors

TFs play an important regulatory role in plant growth and development and defense responses to stress. Our RNA-seq analysis revealed that there were 943 TFs, and the top five TFs included members of the WRKY, MYB, bHLH, NAC, and ERF families (Figure 8A). We compared the detailed trends of expression of the DEGs that encode these five TF families between the RC and SC based on significant levels of expression ($P \leq 0.05$) (Figure 8B). A total of 27 genes in the MYB family differed significantly. Most of the MYB genes were significantly up-regulated in the RC (particularly at 0 and 1 dpi). We found that the gene expression levels of 10 NAC families were significantly up-regulated in the RC compared to the SC. Interestingly, most of the WRKY TFs responses manifested in RC inoculated with *A. alternata* at 0 and 1 dpi, whereas the SC responded to *A. alternata* infection at 1 dpi and 5 dpi. The bHLH and ERF families of TFs also positively responded to *A. alternata* infestation in the RC at the early stage of inoculation.

MYB TFs are involved in many metabolic pathways, and they also play an important role in the phenylpropanoid biosynthetic pathway (Albert et al., 2015; Guo et al., 2017). Combined with the results of a GO analysis (Table S8), four MYB TFs that were involved in phenylpropanoid biosynthesis were noted, and an RT-qPCR analysis showed that they were significantly up-regulated in the infection process. We found the level of expression of *PcMYB63* significantly increased at 1 dpi in the RC, which was 7.5-fold higher than that in the SC (Figure 8C).

4 Discussion

The determinants of *A. alternata* infestation in cherry and the subsequent complex network of responses remain poorly understood. Exploring the key components of these defense responses is critical to producing disease-resistant crops. In the present study, we used transcriptomic and metabolomic approaches to compare the response of two widely different cherry cultivars inoculated with *A. alternata* and explored sensing, signaling, and defense responses in the disease-resistance system of cherry. These results could further our understanding of the mechanism underlying resistance to *A. alternata* infection in cherry.

Plants under biotic or abiotic stress produce ROS, one of the earliest cellular responses after the host successfully recognizes the pathogen (Sagi and Fluhr, 2006). The balance between ROS synthesis and scavenging can ensure the basal metabolism of plant organisms during the process of stress response (Laloi et al., 2007). Here, the H_2O_2 content of cherry leaves infected with *A. alternata* was significantly higher than that of the uninoculated group. Moreover, the H_2O_2 content of the RC was higher than that of the SC at the early stage of pathogen infection. Therefore, the role of H_2O_2 in the RC may be to induce allergic necrosis of host cells, thereby inhibiting the spread of pathogens. The same phenomenon was observed in the interaction between wheat and stripe rust, with ROS found only in resistant cultivars (Wang et al., 2010). SOD can scavenge superoxide free radicals (O_2^-); it cooperates with CAT, POD, and other enzymes to defend against the damage of ROS or other peroxide free radicals to

The phenylpropanoid pathway was reprogrammed, and phenylalanine, tyrosine, and coumarin accumulated significantly in the RC, with coumarin showing obvious inhibitory effects on the growth of *A. alternata* (Figures 7C, D). The coumarin synthesis pathway is a branch of the phenylpropanoid metabolic pathway, and the metabolite coumarin can resist the growth and reproduction of various plant pathogens, thus enhancing plant disease resistance (Kai et al., 2006). The coumarin derivative (5'-hydroxy-aurapten) extracted from *Lotus lalambensis* could inhibit conidial germination of *Aspergillus flavus* at concentration 40 µg/mL (Ali et al., 2021). Gao et al. (2019) found that coumarin can be used as an inducer of plant immune elicitor to induce ROS production and promoted rice blast resistance activity. It has also been reported that the antifungal effect of coumarin compounds is caused by the change of cell membrane permeability (Ayine-Tora et al., 2016). Therefore, coumarin is expected to be an effective natural antifungal agent for cherry. The lignin and flavonoid pathways are two other important branches of the phenylpropanoid biosynthesis pathway. Although phenylalanine had no significant inhibitory effect on *A. alternata* as an upstream metabolite of phenylpropanoid biosynthesis, it appeared to induce changes in downstream genes. We found that genes encoding CAD, POD, CCoAOMT, 4CL, CCR, and COMT were up-regulated, affecting the lignin content and flavonoid pathways, it was suggested that they may play a potential role in the resistance of cherry to *A. alternata*. A similar interaction was observed between rust-resistant maize strain and *Puccinia sorghi* (Kim et al., 2021). Because lignin biosynthesis is associated with cell wall strengthening as a disease-resistance mechanism, and it has a strong ability to scavenge ROS, the free radicals produced during lignin metabolism can simultaneously inactivate fungal cells (Tronchet et al., 2010; Zheng et al., 2021). Our findings supported this finding. Electron microscopy showed that only sporadic hyphae and single conidia were found on the leaves of the RC (Figure 1D). The lignin content of the RC was significantly higher than that of the SC in the early stage of

inoculation (Figure 7B), and the genes involved in cell wall synthesis were highly expressed in the RC at 0 and 1 dpi, potentially explaining why *A. alternata* cannot invade the RC. The main physiological functions of flavonoids are their capacity to act as free radical scavengers and antioxidants. The up-regulation of CHS and FLS, as well as flavonoid accumulation, played a positive role in the resistance of cherry to *A. alternata*. The ROS scavenging capacity of flavonoids has been proposed to protect against pathogens, including *Sclerotinia sclerotiorum* (Ranjan et al., 2019) and *Phytophthora nicotianae* (Sun et al., 2022). These mechanisms may confer resistance against *A. alternata* in cherry.

MYB, NAC, WRKY, ERF, and bHLH are all important regulators of defense responses in plants (Ambawat et al., 2013; Zhu et al., 2017; Yuan et al., 2021). The MYB TFs in some plants enhance the plants defense against diseases by regulating the synthesis of phytoalexins. *VqMYB154* can regulate the accumulation of resveratrol to enhance the resistance of grapevine to pathogens (Jiang et al., 2021). Overexpression of *SlMYB75* regulated JA accumulation in tomato and promoted JA-mediated signaling against *B. cinerea* infection (Liu et al., 2020). Overexpression of grapevine *VvNAC1* in *Arabidopsis* improved resistance to *B. cinerea* and *Hyaloperonospora arabidopsidis* by regulating defense genes (Le Hénanff et al., 2013). Overexpression of *VaWRKY10* in *Arabidopsis thaliana* and *Vitis vinifera* Thompson Seedless enhanced resistance to *B. cinerea* (Wan et al., 2021). Transgenic rice plants overexpressing *OsERF83* showed substantial inhibition of lesion formation following rice blast infection (Tezuka et al., 2018). Overexpression of *OsbHLH057* enhanced disease resistance and drought tolerance in rice (Liu et al., 2022). Our results showed that specific TFs were significantly higher expression in the RC than in the SC. In particular, we found four MYB TFs that were involved in phenylpropanoid biosynthesis were significantly up-regulated. We hypothesized that these TFs may have important regulatory and transport roles in cherry during resistance against *A. alternata* infection. The role of TFs in the disease resistance of sweet

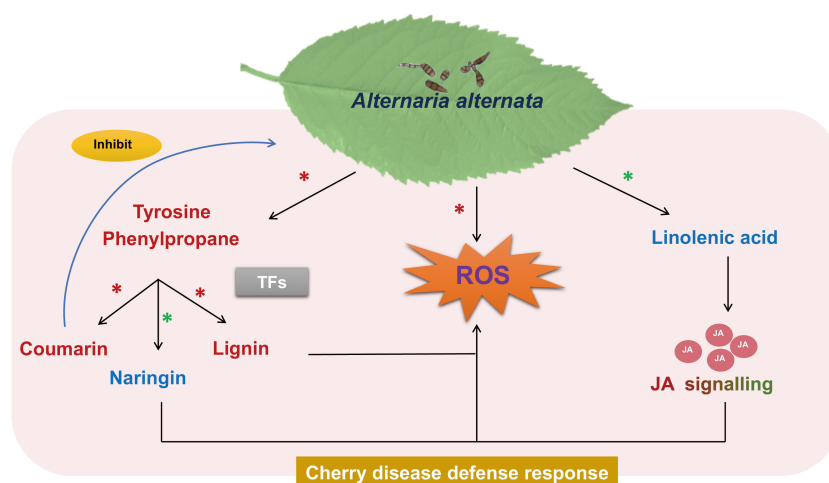


FIGURE 9

The proposed defense response mechanism of cherry to *A. alternata* infection. ROS are the core defense responses of cherry to *A. alternata*; JA, phenylpropanoid, and flavonoid biosynthesis are the key pathways, coumarin could effectively inhibit the growth of *A. alternata*, and TFs could be the key responsive factor in the response of cherry to *A. alternata*. The black line is induction of a process, blue line represents inhibition. Metabolite name indicated in red or blue represent significant accumulation in the RC or SC, respectively. The words indicated by gradient colors, which represent the significant accumulation of JA signaling in RC at an early stage. Red asterisks (*) indicate up-regulation in the resistance response, green asterisks (*) indicate down-regulation in the resistance response.

cherry has not been thoroughly investigated, future work will focus on the in-depth analysis of these TFs to determine their functions.

5 Conclusion

In this study, we proposed a mechanism of the defense response of cherry to *A. alternata* infection (Figure 9). The resistant cultivar exhibited higher antioxidant abilities and stronger cell wall defense at the physiological levels. Transcriptomic and metabolomic analyses revealed the activation of secondary metabolic pathways, including JA, phenylpropanoid, and flavonoid biosynthesis, during the defense responses of cherry against *A. alternata*. The resistance of cherry to *A. alternata* was associated with the early accumulation of JA. Notably, since coumarin could effectively inhibit the growth of *A. alternata*, it is expected to become an available natural antifungal agent for cherry. Moreover, several TFs (e.g., MYB, NAC, WRKY, ERF, and bHLH) that may be involved in *A. alternata*-mediated defense responses by activating disease resistance signaling and downstream defense pathways. Our study provides deeper insights into understanding the mechanisms of resistance of cherry against infection by *A. alternata*.

Data availability statement

The datasets presented in this study can be found in online repositories. The names of the repository/repositories and accession number(s) can be found below: <https://www.ncbi.nlm.nih.gov/>, PRJNA893261.

Author contributions

L-YP, Y-LC and TW conceived and designed the research; L-YP, JiZ, YS, B-XQ, and R-QG performed the experiments; L-YP, JuZ, and

D-QS analyzed the results; L-YP wrote the manuscript; and Y-LC and TW revised the manuscript. All authors contributed to the article and approved the submitted version.

Funding

This work was supported by the Bingtuan Science and Technology Program (Grant number: 2021AB017) and the Agricultural Science and Technology Innovation and Transformation Project of Shaanxi Province [Grant number: NYKJ-2022-YL(XN)47].

Conflict of interest

The authors declare that the research was conducted in the absence of any commercial or financial relationships that could be construed as a potential conflict of interest.

Publisher's note

All claims expressed in this article are solely those of the authors and do not necessarily represent those of their affiliated organizations, or those of the publisher, the editors and the reviewers. Any product that may be evaluated in this article, or claim that may be made by its manufacturer, is not guaranteed or endorsed by the publisher.

Supplementary material

The Supplementary Material for this article can be found online at: <https://www.frontiersin.org/articles/10.3389/fpls.2023.1129515/full#supplementary-material>

References

- Abdelrahman, M., Nakabayashi, R., Mori, T., Ikeuchi, T., Mori, M., Murakami, K., et al. (2020). Comparative metabolome and transcriptome analyses of susceptible *Asparagus officinalis* and resistant wild *A. kiusianus* reveal insights into stem blight disease resistance. *Plant Cell Physiol.* 61 (8), 1464–1476. doi: 10.1093/pcp/pcaa054
- Albert, N. W., Griffiths, A. G., Cousins, G. R., Verry, I. M., and Williams, W. M. (2015). Anthocyanin leaf markings are regulated by a family of R2R3-MYB genes in the genus trifolium. *New Phytol.* 205 (2), 882–893. doi: 10.1111/nph.13100
- Ali, E. M., Alkuwayti, M. A., Aldayel, M. F., and Abdallah, B. M. (2021). Coumarin derivative, 5'-hydroxy-auraptene, extracted from *Lotus lalambensis*, displays antifungal and anti-aflatoxigenic activities against *Aspergillus flavus*. *J. King Saud Univ Sci.* 33 (1), 101216. doi: 10.1016/j.jksus.2020.10.013
- Ambawat, S., Sharma, P., Yadav, N. R., and Yadav, R. C. (2013). MYB transcription factor genes as regulators for plant responses: an overview. *Physiol. Mol. Biol. Plants* 19 (3), 307–321. doi: 10.1007/s12298-013-0179-1
- Ayine-Tora, D. M., Kingsford-Adaboh, R., Asomaning, W. A., Harrison, J. J. E. K., and Reynisson, J. (2016). Coumarin antifungal lead compounds from *milletia thonningii* and their predicted mechanism of action. *Molecules* 21 (10), 1369. doi: 10.3390/molecules21101369
- Bari, R., and Jones, J. D. (2009). Role of plant hormones in plant defence responses. *Plant Mol. Biol.* 69 (4), 473–488. doi: 10.1007/s11103-008-9435-0
- Bhattacharj, K. K., Xie, Q. G., Mantelin, S., Bishnoi, U., Girke, T., Navarre, D. A., et al. (2008). Tomato susceptibility to root-knot nematodes requires an intact jasmonic acid signaling pathway. *Mol. Plant Microbe Interact.* 13 (9), 1205–1214. doi: 10.1094/MPMI-21-9-1205
- Cai, Y., Wang, Y., Qiu, R., Feng, Y., Xue, Z., Wan, T., et al. (2014). A new sour cherry cultivar 'Aode'. *Acta Hort.* 968, 1743–1744. doi: 10.16420/j.issn.0513-353x.2014.08.025
- Cervilla, L. M., Blasco B Fau Ríos, J. J., Ríos Jj Fau Romero, L., Romero L Fau Ruiz, J. M., and Ruiz, J. M. (2007). Oxidative stress and antioxidants in tomato (*Solanum lycopersicum*) plants subjected to boron toxicity. *Ann. Bot.* 100 (4), 747–756. doi: 10.1093/aob/mcm156
- Chen, W., Gong, L., Guo, Z., Wang, W., Zhang, H., Liu, X., et al. (2013). A novel integrated method for large-scale detection, identification, and quantification of widely targeted metabolites: application in the study of rice metabolomics. *Mol. Plant* 6 (6), 1769–1780. doi: 10.1093/mp/sst080
- Cheng, X., Lu, Y. M., Chen, D. L., Luo, C., Li, M. Y., and Huang, C. L. (2019). Pathogen and disease characteristics of marigold black spot in Beijing and surrounding areas. *Plant Pathol.* 68, 689–699. doi: 10.1111/ppa.12994
- Cohn, J., Sessa, G., and Martin, G. B. (2001). Innate immunity in plants. *Curr. Res. Immunol.* 13 (1), 55–62. doi: 10.1016/s0952-7915(00)00182-5
- Dhindsa, R. S., Pamela, P. D., and Thorpe, T. A. (1981). Leaf senescence: Correlated with increased levels of membrane permeability and lipid peroxidation, and decreased levels of superoxide dismutase and catalase. *J. Exp. Bot.* 32 (1), 93–101. doi: 10.1093/jxb/32.1.93

- Ding, L., Xu, H., Yi, H., Yang, L., Kong, Z., Zhang, L., et al. (2011). Resistance to hemibiotrophic *F. graminearum* infection is associated with coordinated and ordered expression of diverse defense signaling pathways. *PLoS One* 6 (4), e19008. doi: 10.1371/journal.pone.0019008
- Dong, N. Q., and Lin, H. X. (2021). Contribution of phenylpropanoid metabolism to plant development and plant-environment interactions. *J. Integr. Plant Biol.* 63 (1), 30. doi: 10.1111/jipb.13054
- Elkomy, M. H. (2014). Comparative analysis of defense responses in chocolate spot-resistant and -susceptible faba bean (*Vicia faba*) cultivars following infection by the necrotrophic fungus *Botrytis fabae*. *Plant Pathol. J.* 30 (4), 355–366. doi: 10.5423/PPJ.OA.06.2014.0050
- Gai, Y., Liu, B., Ma, H., Li, L., Chen, X., Moenga, S., et al. (2019). The methionine biosynthesis regulator *AaMetR* contributes to oxidative stress tolerance and virulence in *Alternaria alternata*. *Microbiol. Res.* 219, 94–109. doi: 10.1016/j.micres.2018.11.007
- Gao, Z., Liu, Q., Zhang, Y., Fang, H., Zhang, Y., Sinumporn, S., et al. (2019). A proteomic approach identifies novel proteins and metabolites for lesion mimic formation and disease resistance enhancement in rice. *Plant Sci.* 287, 110182. doi: 10.1016/j.plantsci.2019.110182
- Gao, L., Wang, Y., Li, Z., Zhang, H., Ye, J., and Li, G. (2016). Gene expression changes during the gummosis development of peach shoots in response to *Lasiodiplodia theobromae* infection using RNA-seq. *Front. Physiol.* 7. doi: 10.3389/fphys.2016.00170
- Glazebrook, J. (2005). Contrasting mechanisms of defense against biotrophic and necrotrophic pathogens. *Annu. Rev. Phytopathol.* 43 (1), 205–227. doi: 10.1146/annurev.phyto.43.040204.135923
- Guo, H., Wang, Y., Wang, L., Hu, P., Wang, Y., Jia, Y., et al. (2017). Expression of the MYB transcription factor gene *BplMYB46* affects abiotic stress tolerance and secondary cell wall deposition in *Betula platyphylla*. *Plant Biotechnol. J.* 15 (1), 107–121. doi: 10.1111/pbi.12595
- Hall, R. D. (2011). Plant metabolomics in a nutshell: Potential and future challenges. *Biol. Plant Metabolomics* 43, 1–24. doi: 10.1002/9781444339956.ch1
- Hu, M. X., Zhong, Y., Huang, M. K., Wang, S., Cheng, Q., and Cheng, Z. M. (2018). Differential expression of 12 NBS-encoding genes in two apple cultivars in response to *Alternaria alternata* f. sp. *mali* infection. *Can. J. Plant Sci.* 98, 279–287. doi: 10.1139/cjps-2017-0117
- Iličić, R., Balaž, J., Ognjanov, V., Jošić, D., Vlajić, S., Ljubojević, M., et al. (2018). Evaluation of cherry cultivar susceptibility to bacterial canker and leaf spot disease. *J. Phytopathol.* 166, 799–808. doi: 10.1111/jph.12763
- Jiang, C., Wang, D., Zhang, J., Xu, Y., Zhang, C., Zhang, J., et al. (2021). *VqMYB154* promotes polygene expression and enhances resistance to pathogens in Chinese wild grapevine. *Hortic. Res.* 8, 151. doi: 10.1038/s41438-021-00585-0
- Kachroo, A., and Kachroo, P. (2009). Fatty acid-derived signals in plant defense. *Annu. Rev. Phytopathol.* 47 (1), 153–176. doi: 10.1146/annurev-phyto-080508-081820
- Kai, K., Shimizu, B., Mizutani, M., Watanabe, K., and Sakata, K. (2006). Accumulation of coumarins in *Arabidopsis thaliana*. *Phytochemistry* 67 (4), 379–386. doi: 10.1016/j.phytochem.2005.11.006
- Khakimov, B., Bak, S., and Engelsens, S. B. (2014). High-throughput cereal metabolomics: Current analytical technologies, challenges and perspectives. *J. Cereal Sci.* 59 (3), 393–418. doi: 10.1016/j.jcs.2013.10.002
- Kim, D., Langmead, B., and Salzberg, S. L. (2015). HISAT: A fast spliced aligner with low memory requirements. *Nat. Methods* 12 (4), 357–360. doi: 10.1038/nmeth.3317
- Kim, S. B., Van den Broeck, L., Karre, S., Choi, H., Christensen, S. A., Wang, G. F., et al. (2021). Analysis of the transcriptomic, metabolomic, and gene regulatory responses to *Puccinia sorghii* in maize. *Mol. Plant Pathol.* 22 (4), 465–479. doi: 10.1111/mpp.13040
- Laloi, C., Stachowiak, M., Pers-Kamczyc, E., Warzych, E., Murgia, I., and Apel, K. (2007). Cross-talk between singlet oxygen- and hydrogen peroxide-dependent signaling of stress responses in *Arabidopsis thaliana*. *Proc. Natl. Acad. Sci. U.S.A.* 104 (2), 672–677. doi: 10.1073/pnas.0609063103
- Lawrence, C. B., Singh, N. P., Qiu, J., Gardner, R. G., and Tuzun, S. (2000). Constitutive hydrolytic enzymes are associated with polygenic resistance of tomato to *Alternaria solani* and may function as an elicitor release mechanism. *Physiol. Mol. Plant Pathol.* 57 (5), 211–220. doi: 10.1006/pmpp.2000.0298
- Le Hénaff, G., Profizi, C., Courteaux, B., Rabenoelina, F., Clément, G., Baillieux, F., et al. (2013). Grapevine NAC1 transcription factor as a convergent node in developmental processes, abiotic stresses, and necrotrophic/biotrophic pathogen tolerance. *J. Exp. Bot.* 64 (16), 4877–4893. doi: 10.1093/jxb/ert277
- Li, G., Wang, Y., Zhang, Z., Chen, Y., and Tian, S. (2022). Mushroom alcohol controls gray mold caused by *Botrytis cinerea* in harvested fruit via activating the genes involved in jasmonic acid signaling pathway. *Postharvest Biol. Technol.* 186, 111843. doi: 10.1016/j.postharvbio.2022.111843
- Liang, C., Wan, T., Wu, R., Zhao, M., Zhao, Y., and Cai, Y. (2020). Resistance analysis of cherry rootstock 'CDR-1' (*Prunus mahaleb*) to crown gall disease. *BMC Plant Biol.* 20 (1), 516. doi: 10.1186/s12870-020-02673-0
- Liu, J., Shen, Y., Cao, H., He, K., Chu, Z., and Li, N. (2022). OsBHLH057 targets the AATCA cis-element to regulate disease resistance and drought tolerance in rice. *Plant Cell Rep.* 41 (5), 1285–1299. doi: 10.1007/s00299-022-02859-w
- Liu, M., Zhang, Z., Xu, Z., Wang, L., and Ren, Z. (2020). Overexpression of *SlMYB75* enhances resistance to *Botrytis cinerea* and prolongs fruit storage life in tomato. *Plant Cell Rep.* 40, 43–58. doi: 10.1007/s00299-020-02609-w
- Livak, K. J., and Schmittgen, T. D. (2002). Analysis of relative gene expression data using real-time quantitative PCR and the $2^{-\Delta\Delta CT}$ method. *Methods* 25 (4), 402–408. doi: 10.1006/meth.2001.1262
- Love, M. I., Huber, W., and Anders, S. (2014). Moderated estimation of fold change and dispersion for RNA-seq data with DESeq2. *Genome Biol.* 15 (12), 550. doi: 10.1186/s13059-014-0550-8
- Mauch, F., Mauch-Mani, B., and Boller, T. (1988). Antifungal hydrolases in pea tissue: II. inhibition of fungal growth by combinations of chitinase and beta-1,3-glucanase. *Plant Physiol.* 88 (3), 936–942. doi: 10.1104/pp.88.3.936
- Ning, T., Nan, C., Nan, H., Wei, D., Chen, Z., and Li, Z. (2018). Comparative metabolomics and transcriptomic profiling reveal the mechanism of fruit quality deterioration and the resistance of citrus fruit against *Penicillium digitatum*. *Postharvest Biol. Technol.* 145, 61–73. doi: 10.1016/j.postharvbio.2018.06.007
- Pan, L., Chen, X., Xu, W., Fan, S., Wan, T., Zhang, J., et al. (2022). Methyl jasmonate induces postharvest disease resistance to decay caused by *Alternaria alternata* in sweet cherry fruit. *Sci. Hortic.* 292, 110624. doi: 10.1016/j.scienta.2021.110624
- Pan, L., Zhao, X., Chen, M., Fu, Y., Xiang, M., and Chen, J. (2020). Effect of exogenous methyl jasmonate treatment on disease resistance of postharvest kiwifruit. *Food Chem.* 305, 125483. doi: 10.1016/j.foodchem.2019.125483
- Panstruga, R., Parker, J. E., and Schulze-Lefert, P. (2009). SnapShot: Plant immune response pathways. *Cell* 136 (5), 978. doi: 10.1016/j.cell.2009.02.020
- Pasquariello, M. S., Patre, D. D., Mastrobuoni, F., Zampella, L., Scortichini, M., and Petriccione, M. (2015). Influence of postharvest chitosan treatment on enzymatic browning and antioxidant enzyme activity in sweet cherry fruit. *Postharvest Biol. Technol.* 109, 45–56. doi: 10.1016/j.postharvbio.2015.06.007
- Perteau, M., Kim, D., Perteau, G. M., Leek, J. T., and Salzberg, S. L. (2016). Transcript-level expression analysis of RNA-seq experiments with HISAT, StringTie and ballgown. *Nat. Protoc.* 11 (9), 1650–1667. doi: 10.1038/nprot.2016.095
- Perteau, M., Perteau, G. M., Antonescu, C. M., Chang, T. C., Mendell, J. T., and Salzberg, S. L. (2015). StringTie enables improved reconstruction of a transcriptome from RNA-seq reads. *Nat. Biotechnol.* 33 (3), 290–295. doi: 10.1038/nbt.3122
- Ranjan, A., Westrick, N. M., Jain, S., Piotrowski, J. S., Ranjan, M., Kessens, R., et al. (2019). Resistance against sclerotinia sclerotiorum in soybean involves a reprogramming of the phenylpropanoid pathway and up-regulation of antifungal activity targeting ergosterol biosynthesis. *Plant Biotechnol. J.* 17 (8), 1567–1581. doi: 10.1111/pbi.13082
- Ravi, I., Sharma, V., Bhardwaj, G., and Kumar, S. (2021). Induction of β -1,3-glucanase and chitinase activity, cloning and their characterization in the defense response of *Cuminum cyminum* plant against the fungal pathogen *Fusarium oxysporum*. *Arch. Phytopathol. Plant Prot* 54 (19–20), 1617–1632. doi: 10.1080/03235408.2021.1932016
- Sagi, M., and Fluhr, R. (2006). Production of reactive oxygen species by plant NADPH oxidases. *Plant Physiol.* 141 (2), 336–340. doi: 10.1104/pp.106.078089
- Schuster, M., and Tobutt, K. R. (2004). Screening of cherries for resistance to leaf spot, *Blumeriella jaapii*. *Acta Hortic.* 663 (663), 239–244. doi: 10.1094/PDIS.2003.87.5.471
- Schwessinger, B., and Ronald, P. C. (2011). Plant innate immunity: perception of conserved microbial signatures. *Annu. Rev. Plant Biol.* 63 (1), 451–482. doi: 10.1146/annurev-arplant-042811-105518
- Sun, M., Li, L., Wang, C., Wang, L., Lu, D., Shen, D., et al. (2022). Naringenin confers defence against *Phytophthora nicotianae* through antimicrobial activity and induction of pathogen resistance in tobacco. *Mol. Plant Pathol.* 23 (12), 1737–1750. doi: 10.1111/mpp.13255
- Tezuka, D., Kawamata, A., Kato, H., Saburi, W., Mori, H., and Imai, R. (2018). The rice ethylene response factor *OsERF83* positively regulates disease resistance to *Magnaporthe oryzae*. *Plant Physiol. Biochem.* 135, 263–271. doi: 10.1016/j.plaphy.2018.12.017
- Thomidis, T., and Tsipouridis, C. (2006). First report of alternaria leaf spot on cherry trees in Greece. *Plant Dis.* 90 (5), 680–680. doi: 10.1094/pd-90-0680c
- Tronchet, M., Balagué, C., Kroj, T., Jouanin, L., and Roby, D. (2010). Cinnamyl alcohol dehydrogenases-c and d, key enzymes in lignin biosynthesis, play an essential role in disease resistance in *Arabidopsis*. *Mol. Plant Pathol.* 11 (1), 83–92. doi: 10.1111/j.1364-3703.2009.00578.x
- Wan, R., Guo, C., Hou, X., Zhu, Y., and Wang, X. (2021). Comparative transcriptomic analysis highlights contrasting levels of resistance of *Vitis vinifera* and *Vitis amurensis* to *Botrytis cinerea*. *Hortic. Res.* 8 (1), 103. doi: 10.1038/s41438-021-00537-8
- Wang, C. F., Huang, L. L., Zhang, H. C., Han, Q. M., Buchenauer, H., and Kang, Z. S. (2010). Cytochemical localization of reactive oxygen species (O_2 and H_2O_2) and peroxidase in the incompatible and compatible interaction of wheat-*Puccinia striiformis* f. sp. *tritici*. *Physiol. Mol. Plant Pathol.* 74 (3–4), 221–229. doi: 10.1016/j.pmpp.2010.02.002
- Wang, J., Liu, W., Zhu, D., Zhou, X., Hong, P., Zhao, H., et al. (2020). A *de novo* assembly of the sweet cherry (*Prunus avium* cv. tietoni) genome using linked-read sequencing technology. *PeerJ* 8, e9114–e9114. doi: 10.7717/peerj.9114
- Wünsch, A., and Hormaza, J. I. (2002). Molecular characterisation of sweet cherry (*Prunus avium* L.) genotypes using peach [*Prunus persica* (L.) batsch] SSR sequences. *Heredity* 89 (1), 56–63. doi: 10.1038/sj.hdy.6800101
- Yang, X., Hu, H., Yu, D., Sun, Z., He, X., Zhang, J., et al. (2015). Candidate resistant genes of sand pear (*Pyrus pyrifolia* nakai) to *Alternaria alternata* revealed by transcriptome sequencing. *PLoS One* 10 (8), e0135046. doi: 10.1371/journal.pone.0135046

Yang, L., Jin, M., Cui, L., Li, T., An, J., Wei, L., et al. (2020). Isolation and identification of the pathogen causing cherry black spot in gansu province. *Guoshu Xuebao* 37 (6), 891–899. doi: 10.13925/j.cnki.gsxb.20190532

Yuan, X., Wang, H., Bi, Y., Yan, Y., Gao, Y., Xiong, X., et al. (2021). ONAC066, a stress-responsive NAC transcription activator, positively contributes to rice immunity against *Magnaprothe oryzae* through modulating expression of *OsWRKY62* and three cytochrome P450 genes. *Front. Plant Sci.* 12. doi: 10.3389/fpls.2021.749186

Yuan, S., Yan, J., Wang, M., Ding, X., Zhang, Y., Li, W., et al. (2019). Transcriptomic and metabolic profiling reveals 'Green ring' and 'Red ring' on jujube fruit upon postharvest *Alternaria alternata* infection. *Plant Cell Physiol.* 60 (4), 844–861. doi: 10.1093/pcp/pcy252

Zheng, L., Lu, G., Pei, W., Yan, W., Li, Y., Zhang, L., et al. (2021). Understanding the relationship between the structural properties of lignin and their biological activities. *Int. J. Biol. Macromolecules* 190, 291–300. doi: 10.1016/j.ijbiomac.2021.08.168

Zhou, K., Hu, L., Li, Y., Chen, X., and Ma, F. (2019). MdUGT88F1-mediated phloridzin biosynthesis regulates apple development and *Valsa* canker resistance. *Plant Physiol.* 180 (4), 2290–2305. doi: 10.1104/pp.19.00494

Zhu, L., Ni, W., Liu, S., Cai, B., Xing, H., and Wang, S. (2017). Transcriptomics analysis of apple leaves in response to *Alternaria alternata* apple pathotype infection. *Front. Plant Sci.* 8. doi: 10.3389/fpls.2017.00022